Asymmetrical Filters for Vision Chips: a Basis for the Design of Large Sets of Spatial and Spatiotemporal Filters

Antonio B. Torralba Jeanny Hérault

Laboratoire des Images et des Signaux (LIS)
Institut National Polytechnique de Grenoble (INPG)
46 avenue Félix Viallet, F-38031 Grenoble Cedex, France
{torralba, herault}@tirf.inpg.fr

Abstract

The problem of actual vision machines on VLSI is the implementation of a large set of linear filters selective to features such as edges, corners, orientations, motion. This procedure requires large arrays of filters with complex structures. In order to reduce the complexity, we propose to implement a simple basis of filters able to generate more complex filters such as oriented quadrature band-pass filters, quadrature wedge filters, velocity tuned filters. The current basis consists of asymmetrical filters implemented with Cellular Neural Networks having only one layer and interactions with four neighbors. We show that this basis generates relevant filters for vision applications and show how the particular structure of the filters basis allows the direct implementation of spatio-temporal filters with a low aditional cost.

1. Introduction

Spatial and spatio-temporal filters are the first stage for most vision architectures. These filters are tuned to different features such as edges, corners, orientations, motion, etc. The filters are usually band-pass spatial filters (Gabor, Gaussian derivatives) and velocity-tuned spatiotemporal filters.

Several VLSI implementations of filters have been proposed [5, 6, 7, 9, 10, 11]. Their main approach consists in implementing a Linear Cellular Neural Network (LCNN) [3, 13] with an impulse response close to the impulse response of a given filter. This approach gives rise to complex structures with several layers or connections to more than four neighbors.

In this paper, we adopt a different approach. We propose a simple basis of filters suitable for cellular architectures (one layer with only four neighbor connections). From this basis of filters, we generate more complex filters (oriented quadrature band-pass, quadrature wedge filters) which are approximated by a linear combination of that basis, Fig. 1. Changing the linear combination of the basis filters allows to tune the architecture to different features. The problem of implementing a particular filter in order to solve a specific vision task is formulated as an optimization problem. Specifically, we look for the combination of the basis filters that optimizes a cost function.

The proposed architecture offers a way to implement spatio-temporal filters (motion-sensors) with a low ad-

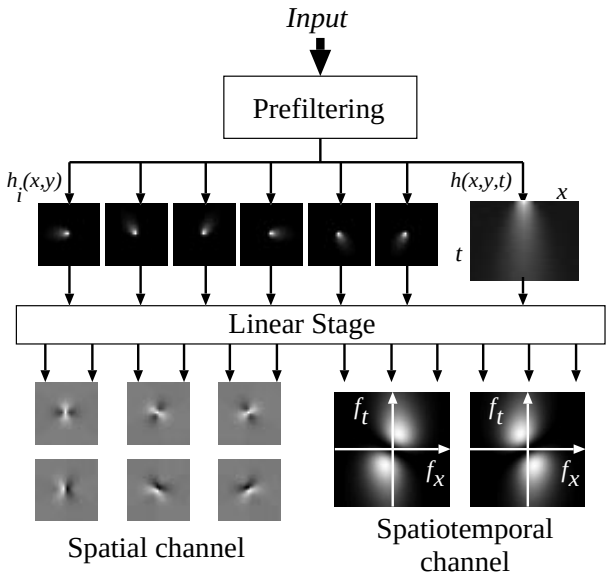

Figure 1. Schema of the architecture using a set of spatial filters and one spatiotemporal filter.

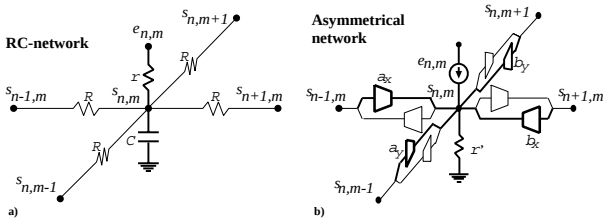

Figure 2. One cell of the a) RC-network and b) Asymmetrical network. Each cell corresponds to one pixel.

ditional cost. This approach opens an issue to the problem of implementing large sets of spatial and spatiotemporal filters tuned to different features (edges, junctions, velocity, ...).

2. Basic LCNN filters

One of the main problems was the choice of a relevant basic set of filters. The complexity constraint imposes to develop filters with few connections. Classical algorithms in vision impose to analyse an image (or a sequence) with a set of filters tuned to different orientations, scales and velocities. Therefore, the complexity constraint is mandatory when a high number of filters is required. In this section we present the two basic filters matched to cellular architectures. These filters are the basic elements of the subsequent sections.

2.1. RC-network

A basic *RC-network* [7, 8] circuit is shown Fig. 2(a) The input is the voltage $e_{n,m}$. The output is the voltage $s_{n,m}$. The output node is connected to its four nearest neighbors by resistors R. The capacitor C gives to the network the temporal behavior. This circuit implements a low-pass spatiotemporal filter.

By applying the Kirchoff currents' law at the output node (n, m), we obtain:

$$e_{n,m}(t) = s_{n,m}(t) + \gamma_s^2[4\,s_{n,m}(t) - s_{n-1,m}(t) - s_{n+1,m}(t) - s_{n,m-1}(t) - s_{n,m+1}(t)] + \tau\, ds_{n,m}(t)/dt \quad (1)$$

with $\gamma_s^2 = r/R$ and $\tau = r\,C$. By applying the Fourier transform to equation (1), we obtain the transfer function. In order to simplify the formulas, we will study the behavior for low spatial frequencies. Therefore, we will use the following approximations: $1-\cos(2\pi f_x) \simeq 2\pi^2 f_x^2$ and $\sin(2\pi f_x) \simeq 2\pi f_x$. We obtain:

$$H(\mathbf{f}_s, f_t) = \frac{1}{1 + 4\pi^2\gamma_s^2\|\mathbf{f}_s\|^2 + j2\pi\tau f_t} \quad (2)$$

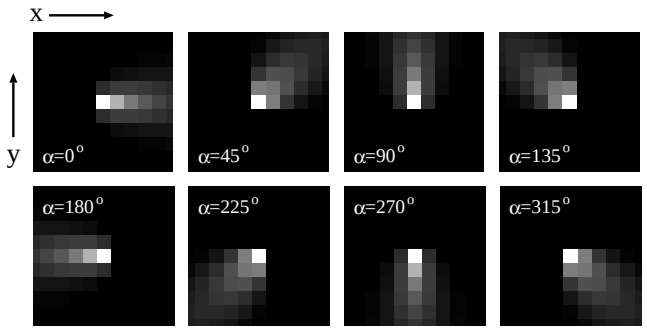

Figure 3. Impulse response of the asymmetrical network for different orientations.

where $\mathbf{f}_s = (f_x,\ f_y)^T$ represents the spatial frequency vector, f_t the temporal frequency. γ_s controls the spatial size (scale) and τ is the time constant of the impulse response for low spatial frequencies. The $-3dB$ spatial bandwidth is $W_s = (3.1\pi\gamma_s)^{-1}$, when $f_t = 0$ and the temporal bandwidth is $W_t = (2\pi\tau)^{-1}$ when $\mathbf{f}_s = (0, 0)$.

2.2. Asymmetrical network

The LCNN shown in Fig. 2(b) implements a spatial oriented filter and it is inspired from a *velocity-tuned* LCNN [15, 16, 17]. In this circuit, "horizontal" resistors have been changed to two unidirectional branches. Each branch has one OTA with variable gain. The input is the current generator $e_{n,m}$ and the output is the voltage $s_{n,m}$. The asymmetrical interactions between output neighbors is responsible of an oriented blurring of the input image. As there is no capacitor, the network implements a pure spatial filter.

By analyzing the circuit, we obtain the next transfer function:

$$H = \frac{1}{1/r' - b_x\, z_x - a_x\, z_x^{-1} - b_y\, z_y - a_y\, z_y^{-1}} \quad (3)$$

The stability condition is [13, 17]:

$$|a_x + b_x| + |a_y + b_y| < 1/r' \quad (4)$$

We can impose $1/r' = 1 + a_x + b_x + a_y + b_y$ in order to have unitary gain at low spatial frequencies.

By defining:

$$\begin{aligned} a_x + b_x &= 2\,\gamma_a^2 \\ a_y + b_y &= 2\,\gamma_a^2 \\ a_x - b_x &= \gamma_a\,\Delta\alpha^{-1}\cos(\alpha) \\ a_y - b_y &= \gamma_a\,\Delta\alpha^{-1}\sin(\alpha) \end{aligned} \quad (5)$$

These definitions gives stability. The low spatial frequency approximation is:

$$H(\mathbf{f}_s) = \frac{1}{1 + 4\pi^2\gamma_a^2\|\mathbf{f}_s\|^2 + j2\pi\gamma_a\,\Delta\alpha^{-1}\,\mathbf{n}^T\mathbf{f}_s} \qquad (6)$$

with $\mathbf{n} = (\cos(\alpha), \sin(\alpha))^T$.

The filter parameters are:

- Spatial scale: γ_a. The maximum spatial bandwidth is $W = (3.1\pi\gamma_a)^{-1}$ and it is obtained when $\mathbf{n}^T\mathbf{f}_s = 0$. Changing the parameter γ_a changes the size of the impulse response of the filter without modifing its shape. For values of $\gamma_a > 0.5$ the LCNN behavior shows little deviation with respect to the low spatial frequency approximation.

- Orientation: α. The input image is more blurred in the direction given by the angle α with respect to the x axis. All the values of $\alpha \in [0, 2\pi)$ are possible.

- Angular resolution: $\Delta\alpha^{-1}$. The larger the value of $\Delta\alpha^{-1}$, the more the image will be blurred in the direction α. $\Delta\alpha$ controls the angular localization of the impulse response.

Orientation selectivity is obtained by means of the complex term in the denominator. Fig. 3 shows the impulse responses of the network for different orientations. The impulse response is that of an oriented low pass filter but with an asymmetrical spatial shape. The asymmetrical shape of the impulse response is the fundamental characteristic of this filter and its relevance will be addressed in the next sections.

We propose to use *asymmetrical networks* as a simple *basis of functions* that would be able to generate interesting filters for the developpement of applications in vision. Symmetrical filters cannot generate the filters we present in next sections and they require more complex architectures (eight neighbors connections in rectangural arrays or six neighbors connections in hexagonal arrays). An efficient implementation of symmetrical oriented filters can be found in [18].

3. Design of spatial band-pass oriented filters

The most appealing filters for spatial vision are quadrature band-pass Gabor filters. Some circuits have been proposed in the literature in order to implement Gabor-type filters [6, 9, 10, 11, 12]. Here, we present a different way to obtain quadrature oriented band-pass filters: rather than using networks that implement oriented band-pass filters, we propose to obtain them as a linear combination of asymmetrical filters yielding to a simpler architecture.

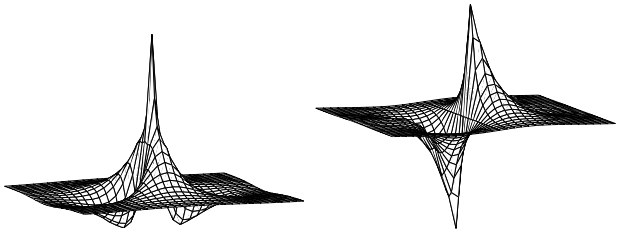

Figure 4. Oriented band-pass filters in quadrature obtained by linear combination of the outputs of six asymmetrical networks.

The starting point is a set of oriented filters implemented by N asymmetrical networks: $\{h_0, h_1, ..., h_{N-1}\}$, where $h_i(\mathbf{x})$ is the spatial impulse response of the asymmetrical network i with the orientation given by the angle $\alpha_i = 2\pi i/N$. $\mathbf{x} = (x, y)^T$ are the spatial variables. We work with continuous spatial variables as we use the low spatial frequencies approximation.

We look for a band-pass filter, $g(\mathbf{x})$, obtained by linear combination of the asymmetrical filters, $h_i(\mathbf{x})$:

$$g(\mathbf{x}) = \sum_{i=0}^{N-1} a_i\, h_i(\mathbf{x}) \qquad (7)$$

where a_i may be complex coeficients. We look for filters optimizing a cost function that represents the desired properties of a band-pass oriented filter. Gabor filters are used to analyze the local orientations in an image. Therefore, we look for a band-pass filter $g(\mathbf{x})$ optimizing the frequency resolution. Optimization is done in the space generated by the filter basis $\{h_0, h_1, ...h_{N-1}\}$. The cost function contains two terms: 1) one measuring the frequency resolution and 2) one measuring the spatial resolution as we are interested in local measurements. We propose the next cost function:

$$J = \int \|\mathbf{f}_s - \mathbf{f}_o\|^2\, |G(\mathbf{f}_s)|^2 d\mathbf{f}_s + \lambda \int \|\mathbf{x}\|^2 |g(\mathbf{x})|^2 d\mathbf{x} \quad (8)$$

being $\mathbf{f}_o = (f_{x_o}, 0)$ the central frequency of the band-pass filter $g(\mathbf{x})$, and

$$f_{x_o} = \frac{1}{E_g} \int f_x\, |G(\mathbf{f}_s)|^2 d\mathbf{f}_s \qquad (9)$$

$$E_g = \int |g(\mathbf{x})|^2 d\mathbf{x} \qquad (10)$$

where $G(\mathbf{f}_s)$ is the Fourier transform of $g(\mathbf{x})$. The first term of equation (8) is the frequency size of the filter,

Table 1. Variation of the central spatial frequency with respect to γ_a

γ_a	0.5	1	2
f_{x_o}	0.25	0.14	0.08

Table 2. Properties of the oriented band-pass filter

	DCR	NFR
6 filters	14 dB	15 dB
8 filters	17 dB	21 dB

the second term is the spatial size. Minimization is done with respect to the complex coeficients a_i. The parameter λ allows us to weight separately the frequency localization and the spatial localization of the spatial filter $g(\mathbf{x})$. Minimization of equation (8), done under the constraint E_g = constant, imposes the magnitude of the transfer function $G(\mathbf{f}_s)$ to be asymmetrical. This implies that the filter $g(\mathbf{x})$ is complex (a_i are complex coefficients). The real and complex parts of $g(\mathbf{x})$ are the approximation of the quadrature pair of band-pass filters. We can add a term of the form $\beta\,|G(0,0)|^2$ to the cost function in order to reduce the throughput of the mean value of the input. The larger the value of β will be, the more we will penalize the mean gain of the filter. However, a large value of β will produce a larger frequency bandwitdth.

Minimization of the cost function (8) can be done numerically by writing the cost function in matrix notation. In order to compute the central frequency f_{x_o} it is necessary to iterate equations (8) and (9).

For example, with $\lambda = 1$ and $\beta = 4$ the coefficients obtained are:

$$Real(a_i) = [-1,\ \ 0.54,\ \ 0.54,\ -1,\ \ 0.54,\ \ 0.54]$$
$$Imag(a_i) = [-0.79,\ \ 1.22,\ -1.22,\ \ 0.79,\ -1.22,\ \ 1.22]$$

The filter parameters are set to $\gamma_a = 1$ and $\Delta\alpha = 2$ for the asymmetrical networks. $\Delta\alpha$ is set in order to have a smooth shape of the function $g(\mathbf{x})$. The spatial scale γ_a will modify the central frequency of the band-pass filter. Table 1 shows the dependency of f_o with respect to γ_a ($f_o \sim 1/\gamma_a$). Figure 4 shows the spatial shape of the impulse response of the band-pass quadrature filters. By rotation of the coefficients a_i we can obtain oriented filters tuned to orientations 30 deg, 90 deg and 150 deg. At the lefthand side of Figure 5, we show the $-3dB$ contour diagram of the magnitude

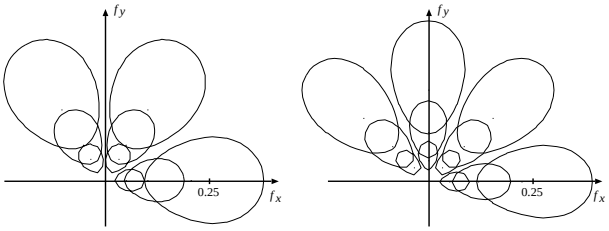

Figure 5. -3dB countour plots of a set of pass-band filters obtained from 6 asymmetrical networks (left) and 8 asymmetrical networks (right) for three spatial scales.

Figure 6. Local energy output for filters with orientations 0 deg and 90 deg obtained from eight asymmetrical networks. The image (70x70 pixels) has been prefiltered in order to eliminate low spatial frequencies.

of the band-pass filters obtained for three spatial scales (table 1) and using six asymmetrical networks at each spatial scale. The righthand side of Figure 5 shows the same but from eight asymmentrical filters. It can be noted that using more asymmetrical networks gives narrower band-pass filters. Figure 6 shows the local output energies for two orientations (addition of the squared output of both phase and quadrature filters).

A basis of filters containing only symmetrical (or only antisymmetrical) filters cannot generate quadrature band-pass filters as they require both symmetrical and antisymmetrical components.

In order to measure the properties of the quadrature pair of band-pass filters, we measure the DC Rejection (DCR) and the Negative Frequency Rejection (NFR). The definitions of the DCR and NFR can be found in [11]. Table 2 shows the results obtained when using 6 and 8 basis filters.

4. Design of spatial Wedge filters

Simoncelli and Farid [14] defined Wedge filters as asymmetrical filters with optimally localized oriented

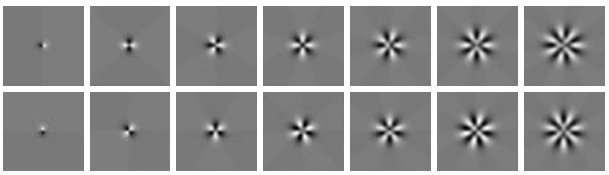

Figure 7. Functions c_n and s_n obtained as a linear combination of asymmetrical filters.

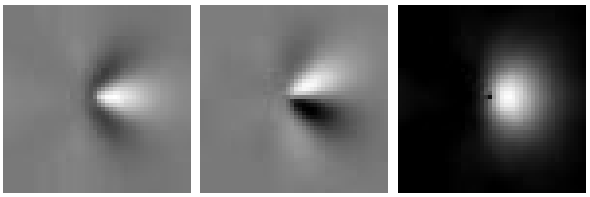

Figure 8. Wedge filters impulse response: in-phase (left), quadrature (center) and asymmetric "local energy" (right) obtained from 10 asymmetrical networks.

energy. Oriented energy map is computed by adding the squared outputs of the phase and quadrature outputs of band-pass filters for each direction of tuning. Gabor filters have a symmetric oriented energy map due to the symmetry and antisymmetry of the phase and quadrature impulse response. Wedge filters are designed to have an asymmetric oriented energy map allowing the identification of junctions.

Simoncelli and Farid constructed the quadrature pair of Wedge filters as:

$$w_e(r,\theta) = g(r) \sum_{n=1}^{N} b_n \cos(n\,\theta) \tag{11}$$

$$w_o(r,\theta) = g(r) \sum_{n=1}^{N} b_n \sin(n\,\theta) \tag{12}$$

These functions are given in polar coordinates: r and θ. $g(r)$ determines the radial shape of the filter's impulse response. The coefficients b_i are calculated in order to obtain the maximal angular resolution. By increasing N we increase the angular resolution but we need more rotated versions of the Wedge filter in order to sample all the orientations. The problem is that the functions $g(r)\cos(n\,\theta)$ and $g(r)\sin(n\,\theta)$ cannot be easily implemented by cellular architectures.

Here, we can obtain an approximation of quadrature Wedge filters as a linear combination of the functions $\{h_0, h_1, ..., h_{N-1}\}$. The cost function associated

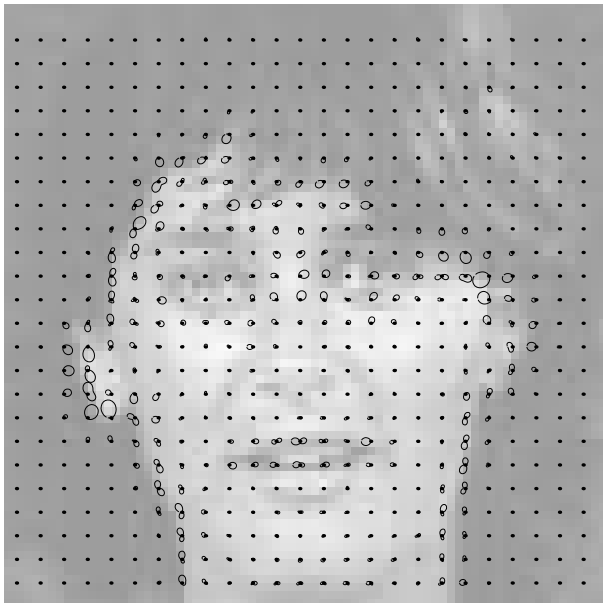

Figure 9. Orientation energy-map obtained from Wedge filters. The Figure shows the polar diagram obtained at each pixel (only one every fourth pixel is shown for clarity). When the image has a symmetric local structure, the polar map is symmetric showing the dominant orientation. When the local structure is asymmetric this is reflected on the polar map.

to Wedge filters is [14]:

$$J = \int_0^{\infty} \int_{-\pi}^{\pi} \theta^2 \left(w_e(r,\theta)^2 + w_o(r,\theta)^2 \right) r\, d\theta\, dr \tag{13}$$

The minimization of this cost function must be done in the space generated by the functions $\{h_0, h_1, ..., h_{N-1}\}$. We propose to change to another basis of functions, more suitable for the minimization problem at hand, figure 7:

$$c_n(r,\theta) = \sum_{i=0}^{N-1} \cos\left(2\pi \frac{n}{N} i\right) h_i(r,\theta) \quad n = 0 ... \frac{N}{2} \tag{14}$$

$$s_n(r,\theta) = \sum_{i=0}^{N-1} \sin\left(2\pi \frac{n}{N} i\right) h_i(r,\theta) \quad n = 1 ... \frac{N}{2} - 1 \tag{15}$$

We assume that N is even (for N odd the limits must be modified). As h_i is asymmetrical, the functions c_n and s_n are non-null. It can be shown that these functions are an orthogonal basis and that the pair c_n and s_n are in quadrature with respect to the angular variable θ. It

must be noted that c_0 is the average of all the rotated versions of the filter used as basis. The other functions, c_n and s_n with $n > 0$ have null mean, Fig. 7. The functions c_n and s_n are approximations of the functions $g(r)\cos(n\,\theta)$ and $g(r)\sin(n\,\theta)$ used by Simoncelli and Farid. Quadrature wedge filters can be approximated as:

$$w_e(r,\theta) = \sum_{n=1}^{N/2-1} b_n c_n(r,\theta) \tag{16}$$

$$w_o(r,\theta) = \sum_{n=1}^{N/2-1} b_n s_n(r,\theta) \tag{17}$$

We ignore the term c_0, as it is low-pass, and the term $c_{N/2}$ as it has not its equivalent counterpart in quadrature ($s_{N/2}$ is null). w_e and w_o are in quadrature because c_n and s_n are in quadrature. Coefficients b_n are obtained by minimization of eq. (13) under the constraint of constant energy. This function can be minimized numerically by using the sampled versions of the functions w_e and w_o in a way similar to that shown in [14].

Once the coefficients b_n are found, the approximation of the Wedge filters can be written as a linear combination of the functions h_i:

$$w_e(\mathbf{x}) = \sum_{i=0}^{N-1} a_i^e\, h_i(\mathbf{x}) \tag{18}$$

$$w_o(\mathbf{x}) = \sum_{i=0}^{N-1} a_i^o\, h_i(\mathbf{x}) \tag{19}$$

Coefficients a_i^e and a_i^o are real. The angular parameter of the asymmetrical networks is set to $\Delta\alpha = 4$. In the case of Wedge filters we will need more orientations than in the case of Gabor filters. Wedge filters require at least 10 asymmetrical networks in order to obtain a wedge filter with a convenient angular resolution.

The coeficients obtained after minimization of J for 10 filters are:

$$a^e = [1,\ -0.26,\ -0.36,\ 0.2,\ -0.14,\ 0.12,\ -0.14,\ 0.2,\ -0.36,\ -0.26] \tag{20}$$

$$a^o = [0,\ 0.8,\ -0.34,\ 0.04,\ -0.01,\ 0,\ 0.01,\ -0.04,\ 0.34,\ -0.8] \tag{21}$$

Coding these coeficients with four bits gives the same performances as real values.

Figure 8 shows the shape of the impulse response of the quadrature Wedge filters. Figure 9 shows one example of local orientation energy maps obtained from Wedge filters implemented with 10 asymmetrical networks. Figure 10 shows the ability of Wedge filters to detect asymmetries in the local structure of the image.

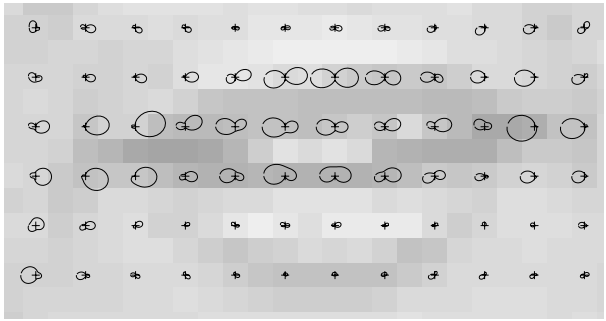

Figure 10. This image shows the detail of the lips from figure 9. At the corners, the polar diagrams are asymmetric. The sign "+" shows the center of each polar energy map.

5. Spatiotemporal nulling filters

Implementation of both spatial vision circuits and spatiotemporal vision circuits require complex and expensive architectures. Maintaining some coherence between the filters used by the spatial vision circuit and by the spatiotemporal vision circuit, the total architecture can be greatly simplified. Here, we propose a way to implement spatiotemporal filters by adding to the previous basis of functions of asymmetrical networks, a unique spatiotemporal filter (the RC-network).

For an input pattern moving with constant velocity, $e(\mathbf{x},t) = e(\mathbf{x} - \mathbf{v}\,t)$, the Fourier transform is:

$$E(\mathbf{f}_s,\, f_t) = E(\mathbf{f}_s)\,\delta(f_t + \mathbf{v}^T\mathbf{f}_s) \tag{22}$$

$E(\mathbf{f}_s)$ is the spatial Fourier transform of the static brightness pattern $e(\mathbf{x})$ and $\delta(.)$ is the Dirac delta distribution. The power of the signal lies on a plane passing through the origin [19] with the equation $f_t + \mathbf{v}^T\mathbf{f}_s = 0$. The output of a spatiotemporal filter $H(\mathbf{f}_s,\, f_t)$ to a moving pattern can be written as:

$$S(\mathbf{f}_s,\, f_t) = E(\mathbf{f}_s)\,H(\mathbf{f}_s, -\mathbf{v}^T\mathbf{f}_s)\,\delta(f_t + \mathbf{v}^T\mathbf{f}_s) \tag{23}$$

appearing as the static input, first filtered by an equivalent spatial filter with transfer function $H(\mathbf{f}_s, -\mathbf{v}^T\mathbf{f}_s)$ and moving at velocity $\mathbf{v}$.

Spatiotemporal nulling filters are filters that have zero response for input patterns moving at one precise velocity [4]. A simple implementation can be obtained by building a nulling filter as: $H_{null}(\mathbf{f}_s,\, f_t) = H(\mathbf{f}_s,\, f_t) - H(\mathbf{f}_s, -\mathbf{v}_{null}^T\mathbf{f}_s) = H(\mathbf{f}_s,\, f_t) - H_s(\mathbf{f}_s)$. Here, the first term is a spatiotemporal filter, $H(\mathbf{f}_s,\, f_t)$, the second term is a spatial filter related to the spatiotemporal filter by the equation: $H_s(\mathbf{f}_s) = H(\mathbf{f}_s, -\mathbf{v}_{null}^T\mathbf{f}_s)$.

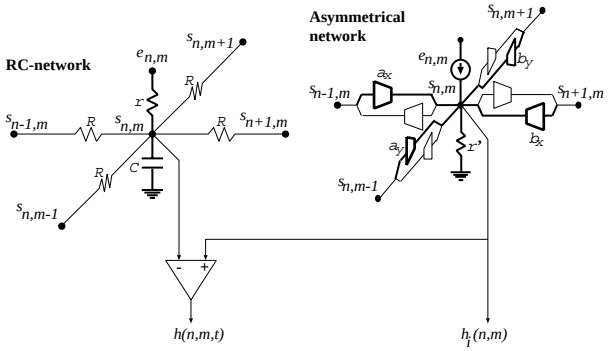

Figure 11. Nulling filter: RC-network (left) and asymmetrical network (right).

The same relation exits between the RC-network and the asymmetrical network (for low spatial frequencies), therefore, they can be used to implement a nulling filter.

The nulling filter, obtained with a low-pass spatiotemporal filter and an asymmetrical oriented filter, will have the transfer function:

$$H_{null}(\mathbf{f}_s,\ f_t) = \frac{1}{1+4\pi^2\gamma^2\|\mathbf{f}_s\|^2 + j2\pi\tau f_t} - \frac{1}{1+4\pi^2\gamma^2\|\mathbf{f}_s\|^2 + j2\pi\gamma\,\Delta\alpha^{-1}\,\mathbf{n}^T\mathbf{f}_s} \quad (24)$$

with $\gamma = \gamma_s = \gamma_a$. The first term of eq. (24) is the transfer function of the RC-network, eq. (2), and the second term is the transfer function of the asymmetrical oriented filter, eq (6). The numerator of the transfer function $H_{null}(\mathbf{f}_s,\ f_t)$ is:

$$j2\pi(\gamma\,\Delta\alpha^{-1}\,\mathbf{n}^T\mathbf{f}_s - \tau f_t) \quad (25)$$

The denominator being responsible of an overall low-pass filter. The nulling velocity of this filter is:

$$\mathbf{v}_{null} = \frac{\gamma}{\tau}\Delta\alpha^{-1}\mathbf{n} \quad (26)$$

The filter obtained is an approximation of a spatiotemporal derivative filter for low spatiotemporal frequencies. Such a filter can be used in the framework of gradient-based algorithms for motion estimation. Nulling can also be an effective procedure to compute motion in presence of transparent motions or to separate sequences into layers [1, 4]. One of the interests of this filter is that it can be obtained with a low additional cost once we have implemented a battery of basis spatial filters. The spatial vision circuit will generate the spatiotemporal vision circuit by adding only one low-pass spatiotemporal filter (RC-network) and some substractors, see Figure 11. Figure 12 ilustrates the behaviour of two nulling filters.

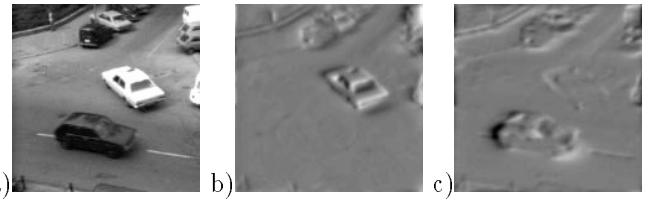

Figure 12. a) Input sequence: "Taxi of Hambourg", there are two moving vehicules. b) and c) are examples of two nulling filter outputs each one nulling the motion of one vehicule.

6. Architecture for spatial and spatiotemporal filtering

The proposed architecture is composed of three stages, see Figure 1. The first stage is the prefiltering [2, 7]. It consists in a high-pass spatiotemporal filter that eliminates the mean value of the input. The second stage is the convolution of the output of the prefiltering with a set of spatial filters and one spatiotemporal filter. Those filters must be as simple as possible in order to allow integration and they must form an interesting *basis of functions* in order to generate filters useful for solving vision tasks. The third stage is the linear combination of the outputs of the filters in order to generate more complex receptive fields better adapted to the visual task to be performed (Gabor filters for local orientation analysis, Wedge filters for junction detection, velocity selective filters for motion estimation, ...). The linear stage will combine outputs at the same pixel. There are no neighbor interactions at this stage.

The architecture proposed is only the first level of a vision module. The next stage will consider non-linear operations as estimation of local oriented energy maps, velocity and direction of motion, junction detection, ...

7. Conclusion

This paper presents the theoretical aspects of an architecture to implement large sets of spatial and spatiotemporal filters. We propose an architecture decomposed in three stages: 1) prefiltering (retina neuromorphic models), 2) filter basis (N spatial filters and one spatiotemporal filter) and 3) design of complex filters by linear combination. The architecture uses a set of filters (obtained by rotations and scalings of a filter h). This approach allows the design of other more complex filters by linear combination (band-pass, wedge, veloc-

ity sensors, ...) without increasing the complexity of the full architecture.

The proposed filter basis is composed of asymmetrical oriented low-pass filters (*asymmetrical network* with nodes connected to its four nearest neigbors). Although the filters presented here are the simplest ones, other filters could be used as basis. For example, *Gabor-Type* filters [10, 11] are also good candidates. As Gabor-Type filters have symmetric and anti-symmetric components, they can also generate other filters such as wedge filters by linear combination but yields to more complex architectures. The choice of the basis filters will be determined by complexity, robustness, noise, non-linear distortion, ...

VLSI implementation of asymmetrical filters can be done using the same technology as that used in [7, 10, 11, 18].

References

[1] E. H. Adelson. Layered representation for image coding. Technical Report 181, Vision and Modeling Group, The MIT Media Lab, December 1991.

[2] W. Beaudot. *Le traitement neuronal de l'information dans la ritine des vertibris.* PhD thesis, INPG, Laboratory TIRF, Grenoble, France, 1994.

[3] L. O. Chua and T. Roska. The CNN paradigm. *IEEE Transactions on Circuits and Systems-I*, 40(3):147–156, 1993.

[4] T. Darrell and E. P. Simoncelli. On the use of "nulling" filters to separate transparent motions. In *Proc. IEEE Conference on Computer Vision and Pattern Recognition*, New York, 1993. IEEE Computer society press.

[5] R. A. Deutschmann and C. Koch. Compact real-time 2-D gradient-based analog VLSI motion sensor. In *Int. conf. on advanced focal plane arrays and electronic cameras*, 1998.

[6] H. Kobayashi, J. L. White, and A. A. Abidi. An active resistor network for gaussian filtering of images. *IEEE Journal of Solid-State Circuits*, 26(5), May 1991.

[7] C. A. Mead and M. A. Mahowald. A silicon model of early visual processing. *Neural Networks*, 1:91–97, 1988.

[8] T. Poggio, V. Torre, and C. Koch. Computational vision and regularization theory. *Nature*, 317(26):314–319, September 1985.

[9] L. Raffo. Resistive network implementing maps of gabor functions of any phase. *Electronics letters*, 31(22):1913–1914, October 1995.

[10] L. Raffo, S. P. Sabatini, G. M. Bo, and G. M. Bisio. Analog VLSI circuits as physical structures for perception in early visual tasks. *IEEE Transactions on Neural Networks*, 9(6), 1998.

[11] B. E. Shi. Gabor-type filtering in space and time with cellular neural networks. *IEEE Trans. on Circuits and Systems-I*, 45(2):121–132, February 1998.

[12] B. E. Shi. A 1D CMOS focal plane array for Gabor-type image filtering. *IEEE Transactions on circuits and systems-I: special issue on bio-inspired processors and CNNs for vision*, 46(2), 1999.

[13] B. E. Shi, T. Roska, and L. O. Chua. Design of linear cellular neural networks for motion sensitive filtering. *IEEE trans. on circuits and systems-II*, 40(5):320–331, May 1993.

[14] E. P. Simoncelli and H. Farid. Steerable wedge filters for local orientation analysis. *IEEE Trans. image processing*, 5(9):1377–1382, September 1996.

[15] A. B. Torralba and J. Herault. From retinal circuits to motion processing: a neuromorphic approach to velocity estimation. In Michel Verleysen, editor, *ESANN'97*, pages 47–54, Brussels, Belgium, April 1997. D facto.

[16] A. B. Torralba and J. Herault. Minimal complexity velocity-tuned filters with analogue neuromorphic networks: A theoretical approach for efficient design. *Neural Processing Letters*, 8(3):229–239, December 1998.

[17] A. B. Torralba and J. Herault. An efficient neuromorphic analog network for motion estimation. *IEEE Trans. on circuits and systems-I: special issue on bio-inspired processors and CNNs for vision*, 46(2), February 1999.

[18] P. Venier, A. Mortara, X. Arreguit, and E. A. Vittoz. An integrated cortical layer for orientation enhancement. *IEEE Journal of solid-state circuits*, 32(2):177–186, 1997.

[19] A. B. Watson and A. J. Ahumada. A look at motion in the frequency domain. In J. K. Tsotsos, editor, *Motion: perception and representation*, pages 1–10, New York, 1983. Association for computing machinery.